Selective hydrogenation of *trans*-cinnamaldehyde over SiO_2-supported Co–Ir bimetallic catalysts

Mingxia Zhu, Xiaoqiang Wang, Jiuyu Lai, and Youzhu Yuan*

State Key Laboratory of Physical Chemistry of Solid Surfaces, Department of Chemistry, Xiamen University, Xiamen 361005, China

Received 17 May 2004; accepted 11 September 2004

Selective hydrogenation of *trans*-cinnamaldehyde was studied on SiO_2-supported Co–Ir bimetallic catalysts. Addition of Ir to Co/SiO_2 increased the hydrogenation selectivity and activity of cinnamaldehyde to the corresponding cinnamyl alcohol (UOL). A selectivity as higher as 93% to UOL at ambient temperature under H_2 pressure of 2.0 MPa was obtained over catalyst with loadings of 10 wt% Co and 0.5 wt% Ir ($Co_{10.0}Ir_{0.5}/SiO_2$). The XRD, Raman and TPR results showed that the higher dispersed Co_3O_4 particles were formed on SiO_2 due to the addition of Ir, which increased the reducibility of Co_3O_4 to Co^0. The reduction of oxidized $Co–Ir/SiO_2$ samples occurred at the temperatures with about 200 K lower than that of the one without Ir species as evidenced by the observations of TPR and *in-situ* Raman characterizations. The XPS results indicated that the large parts of Co_3O_4 in the sample of $Co–Ir/SiO_2$ were reduced to Co^0, but only small parts of that were reduced to Co^0 in the sample of Co/SiO_2 under flowing $5\%H_2/Ar$ at 673 K. The CO chemisorptions revealed that the irreversible uptakes of CO on the reduced $Co–Ir/SiO_2$ sample was much higher than those on the reduced Co/SiO_2 and Ir/SiO_2, and also higher than the combination of that on the reduced Co/SiO_2 and Ir/SiO_2, respectively. The experimental data suggested that the presence of Ir played a key role in the reduction of Co_3O_4 to Co^0 through a strong interaction between them and that the amount of Co^0 at the catalyst surfaces was correlated to the activity and more importantly to the UOL selectivity.

KEY WORDS: selective hydrogenation; *trans*-cinnamaldehyde; bimetallic; Co–Ir; XRD; TPR; Raman; XPS; chemisorption.

1. Introduction

The selective hydrogenation of α, β-unsaturated aldehydes (UAL) containing C=C and C=O groups to the corresponding unsaturated alcohols (UOL) remains a goal of considerable importance both for the industrial production in fine chemicals and for the fundamental research in catalysis [1–6]. Supported Co showed higher hydrogenation selectivity to UOL [7–12]. Nitta *et al.* [7,8] found that the supported Co could efficiently and selectively hydrogenate the carbonyl group of UAL by employing Co loading as high as 40 wt%. They observed a strong selectivity dependence on Co particles size in the liquid phase hydrogenation of cinnamaldehyde. However, Bueno *et al.* reported that there existed at least four different Co surface sites at Co/SiO_2, which affecting the performance for the selective hydrogenation of crotonaldehyde [10,11]. Besides, Several interesting catalysts were effective for the selective hydrogenation of unsaturated aldehydes. For instance, a significant influence of the particle size on the selectivity and activity was found with Ag/TiO_2 and Au/TiO_2 catalysts for the selective hydrogenation of crotonaldehyde [13,14]. Very high selectivities have been reported with electronically promoted catalysts of supported Cu, Ag, Au for the reaction. Gold supported on iron oxide could hydrogenate the citral to the corresponding α, β-unsaturated alcohol with a selectivity higher than 95% [15]. The iron oxide on the catalyst surface could act as a promoter to activate the C=O bond and thus to increase the hydrogenation activity and selectivity. An important enhancement in selectivity could be obtained by the addition of promoters (second metal, oxides or cationic species), through modifying the metal particle size, the structure feature, etc [16]. It has been shown that the bimetallic catalyst Pt–Co exhibited much better catalyst activity and UOL selectivity than the ones Co–Pd and Co–Ru [17–20]. Nevertheless, thus far the detail report on the catalytic selective hydrogenation of unsaturated aldehyde with a bimetallic catalyst Co–Ir is not available.

Trans-cinnamaldehyde, an example of a α, β-unsaturated aldehydes, is of great practical importance [21–24]. Both the hydrogenated and semi-hydrogenated products find wide application in the perfume industry. Besides this, the unsaturated alcohol, cinnamyl alcohol, is an important building block in organic synthesis. Herein we report that a SiO_2-supported bimetallic Co–Ir heterogeneous catalyst which facilitates the chemoselective reduction of cinnamaldehyde to cinnamy alcohol under mild condition.

2. Experimental

2.1. Catalyst preparation

Supported Co–Ir catalysts were prepared by the incipient wetness technique of co-impregnation by sing

*To whom correspondence should be addressed.
E-mail: yzyuan@xmu.edu.cn

1011-372X/04/1200–0247/0 © 2004 Plenum Publishing Corporation

aqueous solutions of H_2IrCl_6 and $Co(NO_3)_2$. After drying by evaporation, the catalysts were dried at 383 K in air for 3 h followed by calcination at 673 K or 4 h under air and reduction at 673 K for 6 h under 5%H_2/Ar with a flow-rate of 30 mL/min, unless otherwise stated. The catalyst was designed as Co_xIr$_y$/support, where x and y stands for the loading weights of Co and Ir atoms (wt%), respectively. Moreover, the catalyst Co_x/Ir_ySiO_2 was prepared by impregnation of H_2IrCl_6 followed by calcination, and then by impregnation of $Co(NO_3)_2$ followed by calcination and reduction, in sequence. The catalyst $Ir_y/Co_x/SiO_2$ was prepared by impregnation of $Co(NO_3)_2$ followed by calcination, and then impregnation of H_2IrCl_6 followed by calcination and reduction, in sequence.

2.2. Characterization

Surface areas of the samples were measured by a BET nitrogen adsorption method at 77 K using a TriStar 3000 machine.

Powder X-ray diffraction (XRD) patterns were recorded with a Rigaku D/Max-C X-ray diffractometer equipped with a rotating anode using Cu K_α radiation ($\lambda = 0.15418$). The anode was operated at 40 kV and 30 mA. The 2θ angles were scanned from 30 to 80 ° at a rate of 2 °/min.

Chemisorption of CO on a series of catalysts was independently determined by static volumetric measurements on a Micromeritics ASAP2010M + C machine. The samples were reduced at 673 K for 4 h under flowing of 5%H_2/Ar, followed by outgassing for 60 min at reduction temperature before allowing them to cool down to the chemisorption temperature at 313 K. The chemisorption isotherm thus obtained was designed as the variation of adsorbed gas quantity as a function of the pressure at equilibrium while maintaining the sample at constant temperature. Chemisorption isotherms were expressed in terms of quantity adsorbed versus absolute pressure. To differentiate the chemisorption from the physisorption contribution, the sample was evacuated after completion of the initial analysis which removed only the reversibly adsorbed gas. Then the analysis was repeated under the same conditions as the original analysis except during the second analysis the active area of the sample was already saturated with chemisorbed molecules. The quantity of CO irreversibly adsorbed by the sample was obtained by subtracting the adsorbed volume data of second analysis from that of initial analysis.

TPR spectra were recorded in the same fixed-bed reaction system equipped with a gas chromatograph. The samples were treated at 473 K for 1 h under flowing of argon and then switched to a reduction gas of 5%H_2/Ar with a flow-rate of 35 mL/min, and heated to 1073 K at a heating rate of 10 K/min for TPR measurements.

The *in-situ* Raman spectra of the samples were recorded on Renishaw-UV–Vis Raman System 1000 by projecting a continuous wave laser of argon ion (Ar^+) green (514.532 nm) by using a *in-situ* lab-made Raman cell. The samples were reduced under flowing of 5%H_2/Ar at different temperatures and then cooled down to 313 K each time under flowing of 5%H_2/Ar to collect the Raman spectra. A scanning range of 200–1000 cm^{-1} with a solution of 2 cm^{-1} was applied.

The X-ray photoelectron spectroscopy (XPS) was measured with a PHI Quantum 2000 Scanning ESCA Microprobe equipment (Physical Electronics) using monochromatic Al K_α radiation ($hv = 1846.6$ eV, 25 W). The background pressure in the analysis chamber was lower than 1×10^{-7} Pa. The X-ray beam diameter was 100 μm, and the pass energy was 58.7 eV for each analysis. The binding energy was calibrated using a C 1s photoelectron peak at 284.6 eV as a reference. The samples of pressed pellets were sealed in a glass tube under high-purity Ar after reduction, then put into the pre-vacuum chamber of the device to avoid the samples contact with air as much as possible. After that, the samples were transferred into the analytical chamber by means of a transfer sledge.

2.3. Catalytic hydrogenation

The catalytic hydrogenation of *trans*-cinnamaldehyde was carried out in a stainless steel autoclave of 60 mL equipped with a magnetic stirrer. After the catalyst, cinnamaldehyde and ethanol were placed in the autoclave, the reactor was filled three times with 1.0 MPa of H_2 to exclude air. Then, the autoclave was heated to a desirable temperature and pressurized with H_2 to 2.0 MPa. Once the pressure reached a steady state, the hydrogenation reaction was initiated immediately by stirring the reaction mixture vigorously (800 rpm). After the reaction, the organic substance was analyzed on a gas chromatograph equipped with FID and a capillary column (OV101, 30 m × 0.25 mm × 0.2 μm).

3. Results and discussion

The metallic cobalt nanoparticles were known to be essentially responsible for the selective hydrogenation of unsaturated aldehyde, while the cobalt-silicate that may be formed during the impregnation was much difficult to be reduced to cobalt nanoparticles [25]. Therefore, the structure feature of support has distinctive effects on the dispersion of cobalt on the catalyst surface and then affects the catalytic performance. We compared the catalytic performance for the selective hydrogenation of cinnamaldehyde over the catalysts of $Co_{10.0}/SiO_2$ reduced at different temperature and $Co_{10.0}Ir_{0.5}$ supported on different supports, respectively. The results are listed in tables 1 and 2. The catalyst reduced at 773 K showed the highest reaction conversion and also UOL selectivity

Table 1
The catalytic performance for selective hydrogenation of cinnamaldehyde over $Co_{10.0}/SiO_2$ reduced at different temperature[a]

Entry	Reduction temperature (K)	Conversion (%)	Selectivity (%)			UOL yield (%)
			SAL	SOL	UOL	
1	623	2.2	30.1	12.7	57.2	1.3
2	673	2.9	33.4	5.2	61.4	1.8
3	773	3.5	30.9	6.9	62.1	2.2

[a]Reaction conditions: Temperature = 323 K, total pressure of H_2 = 2.0 MPa, agitation speed = 800 rpm, ethanol = 6.0 mL, cinnamaldehyde = 0.8 mL, catalysts weight = 180 mg, reaction time = 10 min.

Table 2
The catalytic performance for selective hydrogenation of cinnamaldehyde over supported Ir–Co on catalysts with different carriers at loadings of 10.0 wt% Co and 0.5 wt% Ir (molar ratio of Co/Ir = 65.2)[a]

Support	S_{BET} ($m^2\ g^{-1}$)	Conversion (%)	Selectivity (%)			UOL yield (%)
			SAL	SOL	DOL	
SiO_2	303	15.3	9.5	1.6	88.9	13.6
Al_2O_3	165	6.4	14.4	3.0	82.6	5.3
TiO_2	11	9.5	20.0	2.7	77.3	7.3
ZrO_2	6	7.2	22.6	3.4	74.0	5.3
MCM-41	908	7.3	25.0	4.7	70.3	5.1
AC[b]	638	5.6	27.3	4.2	68.5	3.8
MCNTs[c]	114	8.9	21.2	2.8	76.0	6.8

[a]Reaction conditions are the same as in Table 1.
[b]AC stands for active carbon.
[c]MCNTs stands for multi-wall carbon nanotubes which was obtained by a catalytic ecomposition of CH_4 (see ref. [26]).

than that reduced at 623 K or 673 K, although the differences were not large from each other. Upon addition of small amount of Ir into the $Co_{10.0}/SiO_2$, significant improvements in the conversion and UOL selectivity were obtained as showed in Table 2. The performance of such supported Co–Ir catalyst system was affected by the supports. The Co–Ir supported SiO_2, Al_2O_3, TiO_2, ZrO_2, MCM-41, AC and MCNTs were active in order of the reaction conversion for the supports $SiO_2 > TiO_2 >$ MCNTs $> ZrO_2 \sim$ MCM-41 $> Al_2O_3 >$ AC and also were selective in order of the UOL formation for the supports $SiO_2 > Al_2O_3 > TiO_2 >$ MCNTs $> ZrO_2 >$ MCM-41 $>$ AC. Among them, $Co_{10}Ir_{0.5}/SiO_2$ showed the highest reaction conversion of 15.3% and the selectivity of 88.9% to UOL at 323 K.

The activity of Co–Ir/SiO_2 was increased with increasing Ir amount, but the selectivity to UOL was almost saturated to a plateau close to 90% at 323 K once the addition of 0.5 wt% of Ir to $Co_{10.0}/SiO_2$ as illustrated in Figure 1. There was no significant increase

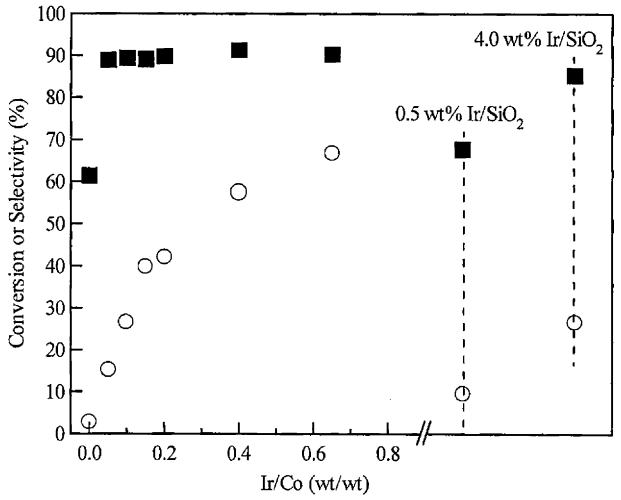

Figure 1. Variations of conversion and UOL selectivity as a function of Ir/Co ratio (wt/wt) in the case of 10.0 wt% Co loading. ○: Conversion; ■: UOL selectivity. Reaction conditions: T = 323 K, time = 10 min; $P(H_2)$ = 2.0 MPa, agitation speed = 800 rpm, ethanol = 6 mL, cinnamaldehyde = 0.8 mL, catalyst weight = 180 mg.

in the formation of UOL but considerable enhancement for the reaction conversion while further addition of Ir into Co/SiO_2 catalysts. On the other hand, the catalysts of Co/SiO_2 or Ir/SiO_2 showed relatively lower conversion and UOL selectivity under identical condition. As for 0.5 wt% Ir/SiO_2 catalyst, a conversion of 9.4% and a UOL selectivity of 67.7% were obtained. As for 4.0 wt% $IrSiO_2$, the conversion and UOL selectivity were slightly increased to 26.6 and 85.3%, respectively. It is worthy noting that the cinnamaldehyde conversion could be increased gradually with negligible influence on the UOL selectivity by prolonging the reaction time.

The cinnamaldehyde conversion was increased drastically by prolonging the reaction time with almost no influence on the UOL selectivity. Figure 2 shows the cinnamaldehyde conversion and the UOL selectivity against the reaction time. The results indicated that the UOL selectivity kept almost unchanged at about 90% when the cinnamaldehyde conversion increased from 15.3 to 64%. Further increase in the cinnamaldehyde conversion caused a small decrease in the UOL selectivity. The UOL selectivity as high as 80.6% was obtained at the cinnamaldehyde conversion of 79.5%.

Figure 3 shows the variations of conversion, product selectivity and UOL yield with $Co_{10.0}Ir_{0.5}/SiO_2$ as a function of reaction temperature. The cinnamaldehyde conversion increased linearly but the UOL selectivity decreased slowly as increasing the reaction temperature. A considerable activity along with a UOL selectivity as high as 93% was obtained at temperatures ranging from 273 to 303 K.

Next we studied the effect of different impregnation sequence on the catalytic performance with the Co–Ir/SiO_2 catalyst. The results in Table 3 indicated that the impregnation sequence was quite sensitive for the

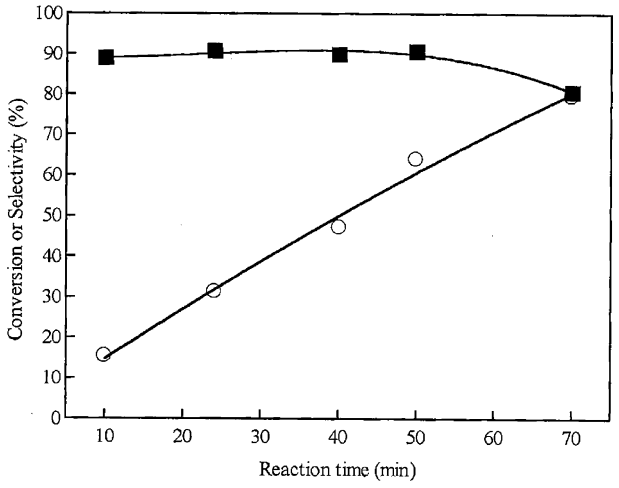

Figure 2. Variations of conversion and UOL selectivity as a function of reaction time with $Co_{10.0}Ir_{0.5}/SiO_2$. ○: Conversion; ■: UOL selectivity. Reaction conditions are the same as in figure 1.

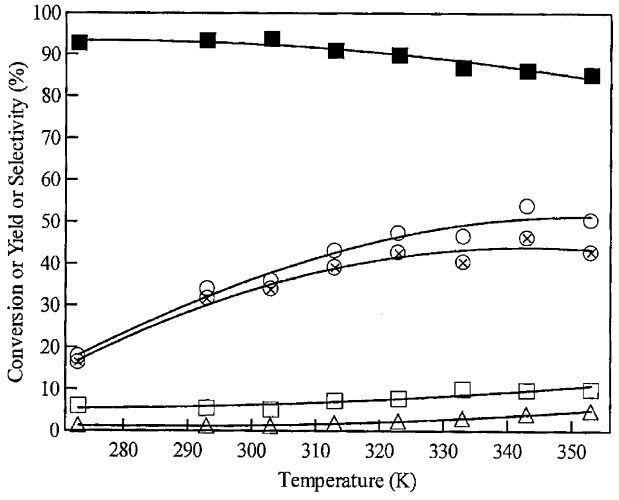

Figure 3. Variations of conversion, selectivity and yield as a function of reaction temperature with $Co_{10.0}Ir_{0.5}/SiO_2$. ○: Conversion; ■: UOL selectivity; □: SAL selectivity; △: SOL selectivity; ⊗ UOL yield. Reaction conditions:time = 40 min; others are the same as in figure 1.

Table 3
The effect of different impregnation sequence on the catalytic performance for selective hydrogenation of cinnamaldehyde

Catalyst	Conversion (%)	Selectivity (%)			Yield (%)
		UOL	SAL	SOL	
$Ir_{2.0}/Co_{10.0}/SiO_2$	21.4	94.4	4.4	1.2	20.2
$CO_{10.0}/Ir_{2.0}/SiO_2$	12.7	92.3	6.3	1.5	11.7
$CO_{10.0}Ir_{2.0}/SiO_2$	42.2	89.8	8.0	2.2	37.9

Reaction conditions: T = 323 k, P = 2 MPa, agitation speed = 800 rpm, ethanol = 6 mL, cinnamaldehyde = 0.8 mL, catalyst = 0.1800 g, time = 10 min.

catalytic activity and selectivity of the $Co_{10.0}Ir_{2.0}/SiO_2$ catalyst. The catalyst derived from co-impregnation afforded the highest activity but the lowest selectivity to UOL, while that derived from adding Co before Ir ($Ir_{2.0}/Co_{10.0}/SiO_2$) showed relatively low conversion but gave the highest selectivity to the UOL.

To obtain the structural information of the catalyst Co–Ir/SiO_2, we carried out the characterizations of X-ray diffraction (XRD) and temperature-programmed-reduction (TPR), *in-situ* Raman spectroscopy and X-ray photoelectron spectroscopy (XPS) for a series of catalysts. Figure 4 shows the XRD patterns for several samples after calcination at 673 K for 4 h under air. There were predominantly existed the diffraction lines typical for cubic Co_3O_4 in the samples of Co/SiO_2 and Co–Ir/SiO_2. No phases for Ir-oxide species were observed for the calcined Co–Ir/SiO_2 samples even if the loading of Ir was as high as 6.5 wt%. The results also showed that the peak intensity for the CO_3O_4 phase in the case of Ir-contained samples was relatively weak but broad, as compared with that for Co/SiO_2. The size of the Co_3O_4 crystallites, as estimated by XRD, tended to decrease from 12 to 8 nm with increasing Ir loading from 0.0 to 6.5 wt%. The results suggested that the dispersion of metal oxides in the samples of Co–Ir/SiO_2 were higher than that for cobalt alone supported on SiO_2. Figure 5 compares the XRD patterns for the catalysts after reduction. As a common feature, the diffraction lines were weak. As for $CO_{10.0}/SiO_2$ catalyst, the cubic phases both for CoO and metallic Co were obtained when the reduction temperatures at 623–673 K, characterizing at about 36.5 °, 42.4 °, 61.5 ° and 44.2 °, 51.5 °(weak), 75.9 °(weak), respectively. More metallic Co could be formed when the reduction temperature was higher (Figure 5a–c), which was beneficial for the selectivity to UOL as evidenced in Table 1. On the other hand, the CoO phase in the

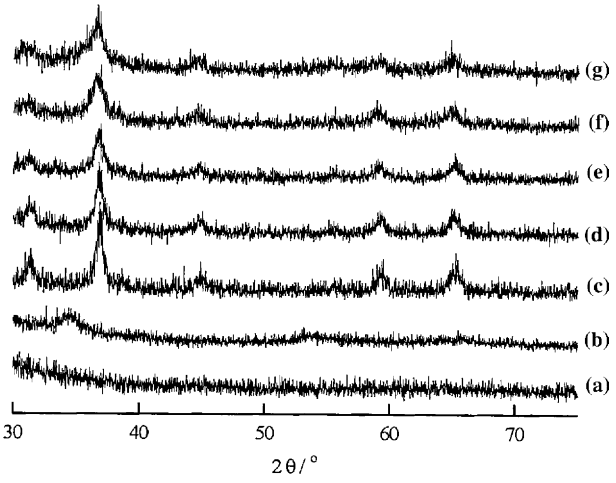

Figure 4. XRD patterns for the samples calcined at 673 K for 4 h. (a) $Ir_{0.5}/SiO_2$; (b) $Ir_{4.0}/SiO_2$; from (c) to (g) for samples $Co_{10.0}Ir_y/SiO_2$: $y = 0$; 0.5; 1.5; 4.0; 6.5.

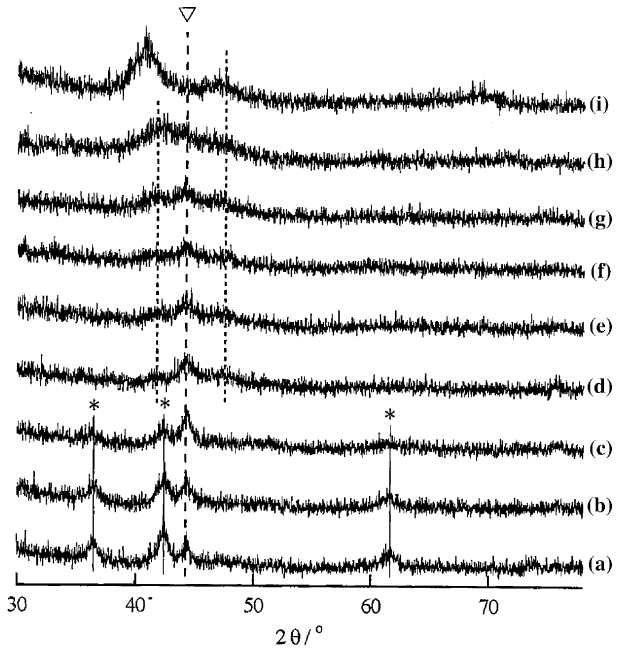

Figure 5. XRD patterns for the samples reduced under flowing of 5%H_2/Ar for 4 h. (a) $Co_{10.0}/SiO_2$ reduced at 623 K; (b) $Co_{10.0}/SiO_2$ reduced at 673 K; (c) $Co_{10.0}/SiO_2$ reduced at 773 K; From (d) to (h) for samples $Co_{10.0}Ir_y/SiO_2$ reduced at 673 K: $y = 0.5$; 1.0; 1.5; 2.0; 4.0; 6.5; (i) $Ir_{4.0}/SiO_2$. ▽: Co^0; ☆: CoO.

samples of Co–Ir/SiO_2 were negligible in the presence of Ir loading ranging from 0.5 to 6.5 wt% (figure 5d). No phases for metallic Ir species were obtained for reduced Co–Ir/SiO_2 catalysts even if the loading of Ir was as high as 6.5 wt%, indicating that the metallic Ir might be embedded into the crystallite phase of metallic Co. Note that the peak at about 47.6 °, accompanying with a broad peak centered at about 41.7 °, was growing up with the Ir content, probably being ascribable to the formation of hexagonal phase of metallic Co.

Figure 6 compares the XRD patterns for the samples obtained with different impregnation sequence before and after reduction. The results were found to essentially similar to each other. While the peak at about 47.6 °, accompanying with a broad peak centered at about 41.7 °, was higher with the samples of $Ir_{2.0}/Co_{10.0}/SiO_2$ (Figure 6e) and $Co_{10.0}/Ir_{2.0}/SiO_2$ (figure 6f) than that with the one by co-impregnation $Co_{10.0}Ir_{2.0}/SiO_2$ (figure 6d). The evidence, along with the results in Table 3, suggested that the Co^0 species ascribable to the formation of hexagonal phase might be related to the selectivity to the UOL.

The results above suggested that the addition of Ir onto Co/SiO_2 caused a higher reducibility of CoO_x and thus the metallic Co was readily formed under the conventional reduction condition. Figure 7 shows the TPR profiles for a series of samples related to Co–Ir/SiO_2 catalysts. The sample $Ir_{0.5}/SiO_2$ showed a hydrogen consumption peak at about 430 K, while the sample $Co_{10.0}/SiO_2$ afforded two peaks at about 620 K and

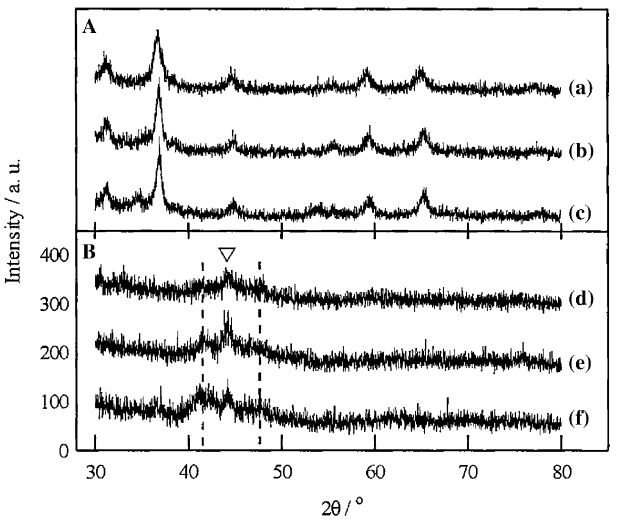

Figure 6. XRD patterns for the samples prepared by different impregnation sequence after (A) calcination under air and (B) reduction at 673 K for 4 h under flowing of 5%H_2/Ar. (a) calcined $Co_{10.0}Ir_{2.0}/SiO_2$; (b) calcined $Ir_{2.0}/Co_{10.0}/SiO_2$; (c) calcined $Co_{10.0}/Ir_{2.0}/SiO_2$; (d) reduced $Co_{10.0}Ir_{2.0}/SiO_2$; (e) reduced $Ir_{2.0}/Co_{10.0}/SiO_2$; (f) reduced $Co_{10.0}/Ir_{2.0}/SiO_2$. ▽: Co^0

680 K respectively. The TPR profile for the oxidized Co/SiO_2 sample was similar to that obtained in literature [10,24]. A drastic different reduction feature, however, was obtained for the samples of Co-lr/SiO_2 as compared to those for Ir/SiO_2 and Co/SiO_2. Essentially there were two hydrogen consumption peaks at about 470–430 K and 590–490 K for the samples contained bimetallic oxides. The two peaks were shifted to the lower temperatures as increasing the Ir content, which coincided with the XRD results. The deconvolution analyses showed that the peak areas at 470–430 K were increased accordingly with the amount of Ir while those at 590–490 K almost kept constant. Therefore, combining with the XRD results, we considered that the

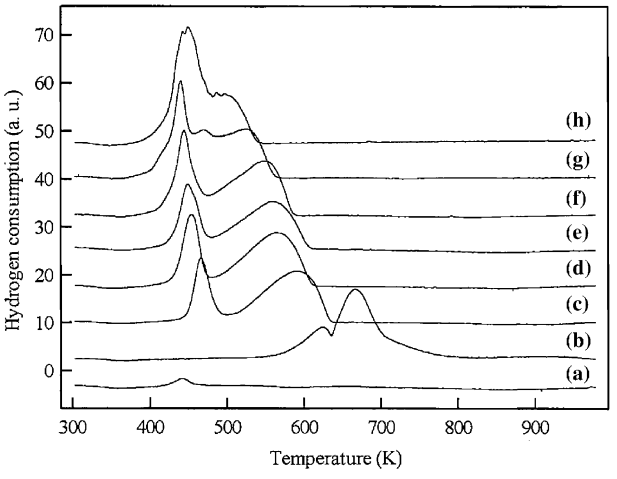

Figure 7. TPR profiles for the catalysts. (a) $Ir_{0.5}/SiO_2$; (b) $Co_{10.0}/SiO_2$; from (c) to (h) for $Co_{10.0}Ir_y/SiO_2$: $y = 0.5$; 1.0; 1.5; 2.0; 4.0; 6.5.

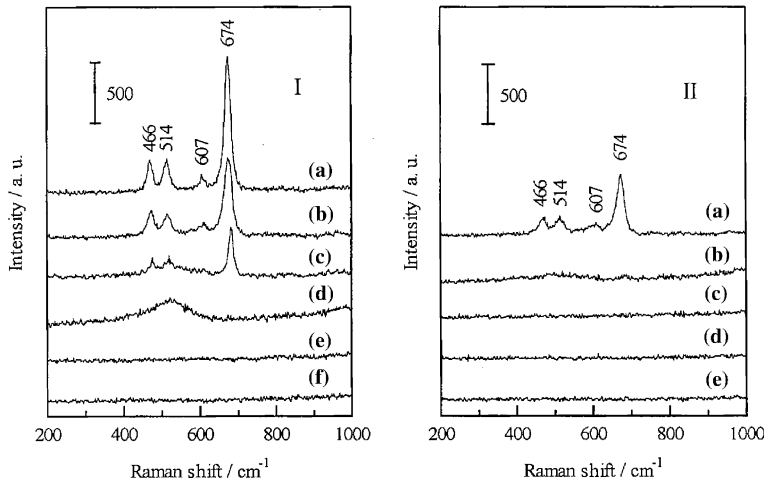

Figure 8. *In-situ* Raman spectra for the as-calcined samples of $Co_{10.0}Ir_y/SiO_2$ during the process of reduction under flowing of $5\%H_2/Ar$ at different temperatures.(I-a) as-received Co_3O_4; (I-b) $Co_{10.0}/SiO_2$ at 298 K; (I-c) $Co_{10.0}/SiO_2$ at 373 K; (I-d) $Co_{10.0}/SiO_2$ at 523 K; (I-e) $Co_{10.0}/SiO_2$ at 573 K; (I-f) $Co_{10.0}/SiO_2$ at 703 K (II-a) $Co_{10.0}.Ir_{0.5}/SiO_2$ at 298 K; (II-b) $Co_{10.0}Ir_{0.5}/SiO_2$ at 373 K; (II-c) $Co_{10.0}.Ir_{0.5}/SiO_2$ at 423 K; (II-d) $Co_{10.0}.Ir_{0.5}/SiO_2$ at 573 K; (II-e) $Co_{10.0}Ir_{0.5}/SiO_2$ at 673 K.

hydrogen consumption peak at 470–430 K might be related to the reduction of IrO_x to metallic Ir, while the peak at 590–490 K was probably due to the reduction of CoO_x to metallic Co. The lower reduction temperature suggested that there might existed a significant synergistic effect between Ir and Co species, which afforded the higher reducibility of cobalt oxides as evidenced in the XRD results.

The *in-situ* Raman spectra for the as-calcined samples of Co_{10}/SiO_2 and $Co_{10}Ir_{0.5}/SiO_2$ during the process of reduction at different temperatures are shown in Figure 8. To identify the Raman bands of the samples, the Raman spectroscopy of Co_3O_4 was collected. The Raman bands of Co_3O_4 exhibited at 674, 607, 514, 466 cm^{-1}, which are similar to the results in literature [27,28]. The Raman spectra of the calcined samples of Co_{10}/SiO_2 and $Co_{10}Ir_{0.5}/SiO_2$ exhibited strong Raman bands at 674, 607, 514, 466 cm^{-1}, which were assigned to Co_3O_4. These results referred to the sample surface, but agreed with the results for material bulk as shown by XRD. When reduction at different temperatures under flowing of $5\%H_2/Ar$, the samples of Co_{10}/SiO_2 and $Co_{10}Ir_{0.5}/SiO_2$ showed rather similar Raman activity, although the temperatures for the structure transformation as reflected by the appearance of Raman bands were different from each other. In the case of Co_{10}/SiO_2, the bands of Co_3O_4 remained after reduction at 373 K. A broad Raman band between 400 and 650 cm^{-1} was emerged when the temperature at 523 K. The broad Raman band was not identical to those of Co_3O_4 or CoO [27,28]. It is suggested that the broad Raman band represented a surface Co compound species related to Co strongly interacting with the silica oxide, likely Co-silicate, which might be formed by Co atom migration into the silicas matrix and was detectable using Raman spectroscopy but not XRD. When the sample was reduced at 573 K, the Raman bands of Co_3O_4 and Co-silicate were totally disappeared. In the case of $Co_{10.0}Ir_{0.5}/SiO_2$, however, the bands of Co_3O_4 disappeared with the reduction temperature at 423 K. The Raman spectroscopy provided additional results with the Co species present, which were in good agreement with the results of XRD and TPR.

Figure 9 shows the Co 2p XPS spectra for the catalysts of $Co_{10}Ir_y/SiO_2$ ($y = 0$, 0.5, 2, 4) reduced at 673 K under flowing of $5\%H_2/Ar$. The Co2p XPS

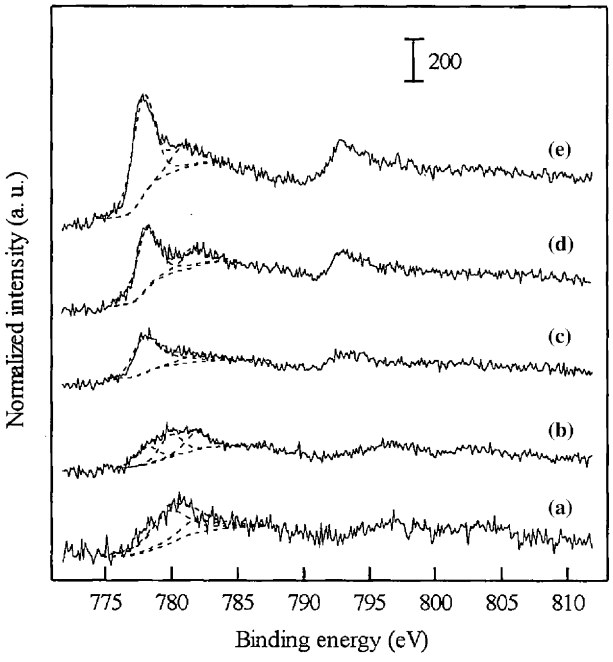

Figure 9. Co 2p XPS spectra for the $Co_{10.0}Ir_y/SiO_2$ catalysts. (a) as-calcined $Co_{10.0}/SiO_2$; from (b) to (e) for the samples $Co_{10.0}Ir_y/SiO_2$ (y = 0.0; 0.5; 2.0; 4.0) reduced at 673 K for 4 h.

Table 4
Deconvolution results of Co $2p_{3/2}$ XPS spectra for the $Co_{10}Ir_y/SiO_2$ samples (y = 0, 0.5,2.0,4.0)

Catalyst	Co^{III}			Co^{II}			Co^0			Co^0 (%)[b]
	B.E. (eV)	FWHM[a] (eV)	Peak area	B.E. (eV)	FWHM[a] (eV)	Peak area	B.E. (eV)	FWHM[a] (eV)	Peak area	
Calcined Co_{10}/SiO_2	779.8	3.2	670.0	781.8	3.1	325.0	–		–	0
Co_{10}/SiO_2	779.9	2.1	229.7	781.9	2.0	217.5	778.0	2.0	173.5	28
$Co_{10}Ir_{0.5}/SiO_2$	–	–	–	781.5	2.4	145.7	777.9	2.1	626.1	81
$Co_{10}Ir_{2.0}/SiO_2$	–	–	–	781.6	2.0	243.4	778.0	2.0	760.1	76
$Co_{10}Ir_{4.0}/SiO_2$	–	–	–	781.7	2.4	269.9	777.9	2.0	1115.5	81

[a]B.E. and FWHM denote binding energy and full width at half maximum, respectively.
[b]Reduction degree (%).

spectroscopy for as-calcined Co_{10}/SiO_2 was also provided in figure 9. The decomposition of the Co 2p spectroscopy for the as-calcined Co_{10}/SiO_2 contained the contribution of Co^{III} and of Co^{II} species. The binding energies in Table 4 for as-calcined Co_{10}/SiO_2 are in good agreement with that in literature [29]. The surface area ratio of the Co $2p_{3/2}$ peaks of Co^{III} and Co^{II} was near to 2, corresponding to the $Co^{II}(Co^{III})2O_4$ formula. The deconvolution of Co $2p_{3/2}$ and Co $2p_{1/2}$ peaks permitted to estimate the reduction degree of outer layer cobalt species (% Co^0) for the reduced samples of $Co_{10}Ir_y/SiO_2$ ($y = 0, 0.5, 2, 4$). The results are reported in Table 4. For the Co_{10}/SiO_2, the amount of cobalt metal was low (28%) and the Co^{III} contribution was still present after reduction at 673 K. For the reduced $Co_{10}Ir_y/SiO_2$ ($y = 0.5$, 2, 4) samples, the amount of cobalt metal was higher (76~81%) and the Co^{III} contribution was no longer present. The Ir $4f_{7/2}$ and Ir $4f_{5/2}$ bands (not shown) appeared at binding energies of 60.6 and 63.6, respectively, for the samples $Co_{10}Ir_y/SiO_2$ (y = 0.5, 2, 4) after reduction at 673 K, which are the values typical of Ir^0. The estimated extent of reduction of the Co_3O_4 phase might provide an evidence for the assistance of Ir^0 in the reduction of Co-ions.

The isotherms for CO adsorption at 313 K on the $Co_{10.0}/SiO_2$, $Ir_{0.5}/SiO_2$, and $Co_{10.0}Ir_y/SiO_2$ ($y = 0.5, 1.0, 4.0, 6.5$) catalysts after reduction at 673 K under flow of $5\%H_2/Ar$ are displayed in Figure 10. Almost no irreversible CO adsorption at 313 was detected on the Co/SiO_2. The irreversible CO adsorption on the $Ir_{0.5}/SiO_2$ was quite small but detectable. Significant CO chemisorption on $Co_{10.0}Ir_y/SiO_2$ ($y = 0.5, 1.0, 4.0, 6.5$) was obtained and the amount was increased as a function of Ir loadings. Such amount of CO adsorbed on the $Co_{10.0}Ir_y/SiO_2$ was not simply due to the combination of that independently on Co/SiO_2 and Ir/SiO_2.

Therefore, addition of small amount of Ir into the SiO_2-supported cobalt system resulted in a strong interaction between the bimetallic species, which resulted in a higher reducibility and thus enhanced the performance of $Co–Ir/SiO_2$ catalyst for the selective hydrogenation of *trans*-cinnamaldehyde to the corresponding cinnamyl alcohol under the mild condition.

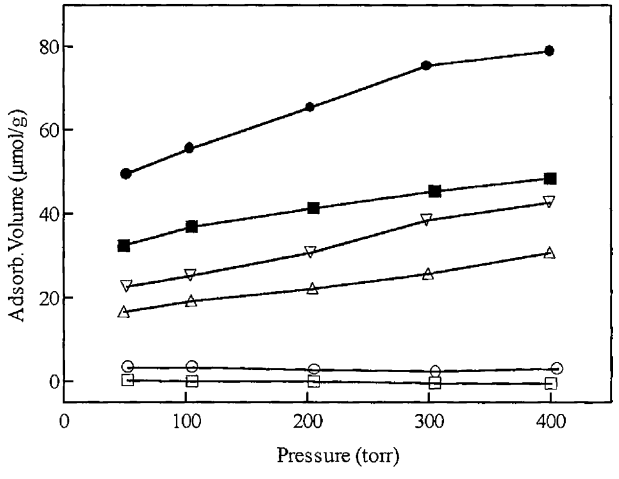

Figure 10. Isotherms for CO adsorption on the catalysts reduced at 673 K under flowing of $5\%H_2/Ar$. □: $Co_{10.0}/SiO_2$; ○: $Ir_{0.5}/SiO_2$; △: $Co_{10.0}Ir_{0.5}/SiO_2$; ▽: $Co_{10.0}Ir_{1.0}/SiO_2$; ■: $Co_{10.0}Ir_{4.0}/SiO_2$; ●: $Co_{10.0}Ir_{6.5}/SiO_2$.

Acknowledgments

This work was supported by the National Natural Science Foundation of China (No. 20021002) and MOE of China.

References

[1] P. Gallezot and D. Richard, Catal. Rev. -Sci. Eng. 401 (1998) 81.
[2] A. Caoma, L.T. Nemeth, M. Renz and S. Valencia, Nature 412 (2001) 423.
[3] K. Baucer and D. Garbe in *Ullman Encyclopedia* (VCH, New York, 1988) All pp. 141.
[4] K. Weissermel and H.J. Arpe, *Industrial Organic Chemistry* (weinheim, Verlag Chemie, 1978).
[5] P. Claus, Top. Catal. 5 (1998) 51.
[6] M. De bruyn, S. Coman, R. Bota, V.I. Parvulescu, D.E. De Vos and P.A. Jacobs, Angew. Chem. Int. Ed. 42 (2003) 5333.
[7] Y. Nitta, K. Ueno and T. Imanaka, Appl. Catal. 56 (1989) 9.
[8] Y. Nitta, Y. Hiramatsu and T. Imanaka, J. Catal. 126 (1990) 235.

[9] C. Ando, H. Kurokawa and H. Miura, Appl. Catal. A: Gen. 185 (1999) L181.
[10] E.L. Rodrigues and J.M.C. Bueno, Appl. Catal. A: Gen. 232 (2002) 147.
[11] E.L. Rodrigues and M.C. Bueno, Appl. Catal. A: Gen. 257 (2004) 201.
[12] E.L. Rodrigues, A. Jmarchi, C.R. Apestequia and J.M.C. Bueno, Stud. Surf. Sci. Catal. 130 (2000) 2087.
[13] P. Claus and H. Hofmeister, J. Phys. Chem. B 103 (1999) 2766.
[14] R. Zanella, C. Louis, S. Giorgio and R. Touroude, J. Catal. 223 (2004) 328.
[15] C. Milone, M.L. Tropeano, G. Gulino, G. Neri, R. Ingoglia and S. Galvagno, Chem. Com. 8 (2002) 868.
[16] V. Ponec, Appl. Catal. A: Gen. 149 (1997) 27.
[17] P. Fouilloux, Stud. Surf. Sci. Catal. 41 (1988) 123.
[18] Z. Zsoldos and L. Guczi, J. Phys. Chem. B 95 (1991) 798.
[19] Z. Zsoldos and L. Guczi, J. Phys.Chem. B 96 (1992) 9393.
[20] B. Liu, G. Xiong, X. Pan, S. Sheng and W. Yang, Chinese J. Catal. 23 (2002) 481.
[21] M.B. Kizling, C. Bigey and R. Touroude, Appl. Catal. A: Gen. 135 (1996) L13.
[22] P. Gallezot, A. Giroir-fendler and D. Richard, Catal. Lett. 5 (1990) 169.
[23] A. Giroir-fendler, D. Richard and P. Gallezot, Catal. Lett. 5 (1990) 175.
[24] Z. Poltarzewski, S. Galvagno, R. Pietropaolo and P. Staiti, J. Catal. 102 (1986) 190.
[25] E. van Steen, G.S. Sewell, R.A. Makhothe, C. Micklethwaite, H. Manstein, M. de Lange and C.T. O'Connor, J. Catal. 162 (1996) 220.
[26] P. Chen, H.B. Zhang, G.D. Lin, Q. Hong and K.R. Tsai, Carbon 35 (1997) 1495.
[27] B. Jongsomjit, J. Panpranot and J.G. Goodwin Jr, J. Catal. 204 (2001) 98.
[28] B. Jongsomjit, C. Sakdamnuson, J.G. Goodwin Jr, and P. Praserthdam, Catal. Lett. 94 (2004) 209.
[29] B. Ernst, S. Libs, P. Chaumette and A. Kiennemann, Appl. Catal. A: Gen. 186 (1999) 145.